Journal of
Ceramic Science
and Technology

J. Ceram. Sci. Technol., **09** [1] 29-36 (2018)
DOI: 10.4416/JCST2017-00054
available online at: http://www.ceramic-science.com
© 2017 Göller Verlag

Influence of the Oxygen Flow Rate on Gas Flow Sputtered Thermal Barrier Coatings

N. Rösemann*[1], K. Ortner[2], M. Bäker[1], J. Petersen[2], G. Bräuer[3], J. Rösler[1]

[1]Institute for Materials, TU Braunschweig, Langer Kamp 8, D-38106 Braunschweig, Germany
[2]Fraunhofer Institute for Surface Engineering and
Thin Films IST, Bienroder Weg 54 E, D-38108 Braunschweig, Germany
[3]Institute for Surface Technology, TU Braunschweig,
Bienroder Weg 54 E, D-38108 Braunschweig, Germany
received July 8, 2017; received in revised form August 8, 2017; accepted September 14, 2017

Abstract

Porous thermal barrier coatings (TBC) reduce the thermal load of gas turbine components. State-of-the-art TBCs consist of partially yttria-stabilized zirconia (PSZ) and are deposited by means of thermal spray techniques or electron beam physical vapor deposition. In this paper, an alternative, innovative deposition technique (reactive gas flow sputtering – GFS) is investigated and the influence of process parameters on the microstructure and the suitability of GFS coatings as TBCs is discussed. PSZ coatings were deposited on polished FeCrAlY-alloy substrates, with varying substrate temperature and oxygen flow rate, and characterized by means of SEM, and XRD.

The substrate temperature is the crucial parameter. Between 500 and 800 °C, four types of columnar microstructures are found based on XRD pattern and morphology. The growth direction of the columns changes from <111> to <100>, accompanied by a change in shape from triangular to four-sided. Varying the oxygen flow rate at a given substrate temperature alters the microstructure defined by the substrate temperature. While oxygen flow rates above a certain level do not have an effect, low oxygen flow rates lead to further densification and compressive stresses, rendering these conditions unsuitable for TBC manufacturing.

In conclusion, promising microstructures are presented accompanied by guidelines for process parameters.

Keywords: Thermal barrier coatings, microstructure, oxygen flow rate, gas flow sputtering

I. Introduction

In modern gas turbines, hot gas temperatures may exceed 1500 °C [1], enabling high efficiencies [2]. Since state-of-the-art nickel-based superalloys sustain temperatures up to ~1100 °C [3], the turbine blades under highest thermal load are internally cooled and protected by a coating system. A metallic bond coat (usually PtAl or MCrAlY) is applied onto the superalloy, enabling oxidation resistance and protection against hot gas corrosion. On top of this, a ceramic thermal barrier coating (TBC) lowers the temperature prevailing at the superalloy. The demands on the TBC are complex and partly contradictory. Zirconia is the most commonly used material [4], featuring a low thermal conductivity and a relatively high coefficient of thermal expansion (for a ceramic). Pure zirconia cannot be used owing to phase transformations under service conditions, which result in volume changes and may cause coating failure. To suppress phase transformations, oxides are added, yttria being the most widely used [5]. With 4 – 4.5 mol% yttria, the metastable t´-phase can be stabilized (PSZ – partially stabilized zirconia) between room temperature and 1200 °C, while higher amounts (> 8 mol%)result in fully stabilized zirconia (FSZ) where the cubic phase is present. Although FSZ allows for higher temperatures, PSZ is state of the art, exhibiting a superior cyclic lifetime and erosion resistance [6 – 8].

TBCs are usually deposited by means of either atmospheric plasma spraying (APS) or electron beam physical vapor deposition (EB-PVD). APS coatings are cost-effective and feature a lamellar microstructure at the cost of no chemical bonding, but feature a shorter lifetime under thermal cycling [9, 10]. The EB-PVD process requires a high vacuum and exhibits lower deposition rates, but the columnar coatings exhibit superior strain tolerance and lifetime [9].

Recently, progress has been made to achieve columnar microstructures without the need for a high vacuum. Suspension plasma spraying (SPS) and plasma spray physical vapor deposition (PSPVD) are two prominent examples [11].

Another approach is to utilize the gas flow sputter (GFS) technique which was first described by Ishii *et al.* [12] for metallic coatings and later expanded for oxide coatings [13]. In a fine vacuum, an intensive hollow cathode glow discharge is established to sputter a metallic target. The sputtered atoms are then transported by a directed inert gas

* Corresponding author: n.roesemann@tu-bs.de

flow towards the substrate where film growth takes place. Upstream of the target, oxygen is fed, enabling the deposition of oxide coatings. Our aim is to evaluate if the GFS coatings can be used as TBCs. In a first step the influence of critical process parameters on the resulting microstructure has to be understood. In previous studies [14,15], we have shown that promising columnar microstructures can be deposited and that the substrate temperature influences the adatom mobility, resulting in decreased porosity at higher temperatures. Surface diffusion has been determined to be the main physical principle concerning the crystal growth. Additionally, a growth model linking different morphologies with growth direction of the columns was presented.

A given microstructure can be altered systematically by argon ion bombardment induced by a negative bias voltage. While low bias voltages promote more regular columns, high bias values result in dense coatings unsuitable for the use as TBCs [16].

Although being an easy accessible parameter, the influence of the oxygen flow rate on the microstructure has yet to be studied in detail. Further insights may be beneficial to tailor a superior microstructure for the use as TBC. In order to do so, the second aim of this paper is to give general guidelines for the process parameters to deposit suitable GFS TBCs.

II. Experimental

Zirconia coatings with a thickness of approximately 50 µm are deposited on cuboid (115 mm x 14 mm 2.5 mm) substrates of the commercial FeCrAlY-alloy Kanthal AF. In this model system, the FeCrAlY-alloy is used as a substitute for a NiCrAlY bond coat. FeCrAlY exhibits similar oxidation behavior, but does not undergo phase transformations at deposition temperatures, rendering it suitable for the focused study of the microstructural evolution of the TBC. Prior to deposition, the substrates are polished and wet-chemically cleaned.

The zirconia coatings are deposited in a cylindrical recipient (see Fig. 1) where a working pressure of 0.2 to 0.3 mbar is maintained by a roots vacuum pump and a rotary vane pump. The substrate (1) can oscillate linearly in the oven (2) above the sputter source. Sputtered species can enter the oven through a hole (3) which is coaxially aligned to the sputter source. The oven can be sealed with a shutter (4), enabling a defined start of the sputter process. During the process, the substrate temperature is monitored by a thermocouple attached to the backside of the substrate (5). Between the oven and the sputter source, oxygen is fed through a tubular die (6).

The sputter source is tubular and made of a ZrY alloy (92.4 at% Zr and 7.6 at% Y), which results in a 4 mol% yttria PSZ coating after stoichiometric oxidation. 3 slm argon are fed through the source allowing for DC plasma excitation (5 kW) and the transport of the sputtered species towards the substrate.

To study the influence of the oxygen flow rate, it was varied between 5 sccm and 200 sccm at three different substrate temperatures (500 °C, 650 °C, 800 °C), compare Table I. The morphology of the resulting coatings was analyzed in top views, fracture surfaces and polished cross-sections utilizing scanning electron microscopy (SEM; Zeiss DSM982 Gemini).

To gain further insights into the microstructure, selected samples were examined with the focused ion beam (FIB) technique (FEI Helios NanoLab 650 SEM). The geometrical deposition rate was determined by dividing the coating thickness (measured with optical light microscopy in polished cross-sections at 15 different positions) by the deposition time. The preferential grain orientations and phases were measured in Bragg-Brentano geometry with X-ray diffraction measurements in a Philips X'Pert Pro MRD diffractometer with a CuKα source.

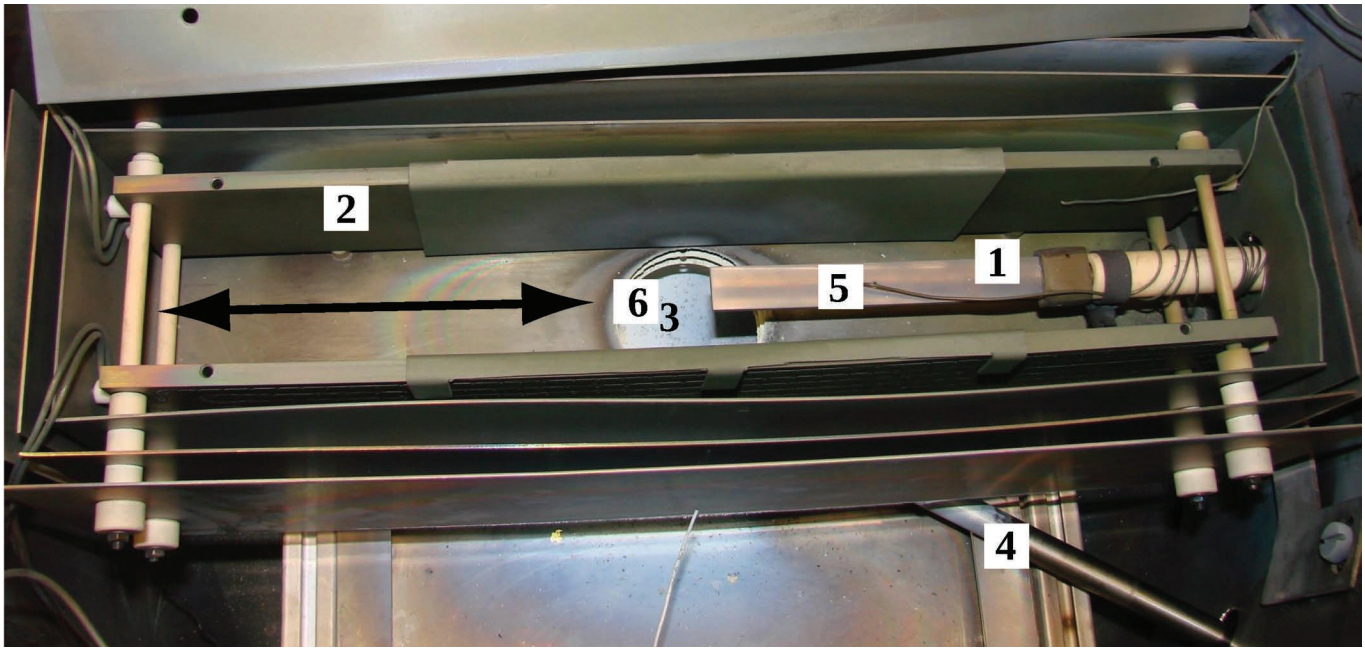

Fig. 1: The inside of the vacuum chamber. 1: Substrate which can be moved linearly (indicated by the arrow). 2: Oven (consisting of the heater and three layers of thermal insulation sheets). 3: Hole in the oven through which the sputtered species enters. 4: Shutter. 5: Thermocouple. 6: Oxygen feed.

Table I: Summary of the sample parameters. The other process parameters are held constant: working pressure: 0.2 to 0.3 mbar; discharge power: 5 kW; argon flow rate: 3 slm.

Sample	Substrate temperature	Oxygen flow rate [sccm]	Deposition time [s]
A	650 °C	5	9900
B	650 °C	10	9900
C	650 °C	20	9900
D	650 °C	50	9900
E	650 °C	100	9900
F	650 °C	150	9900
G	500 °C	10	9900
H	500 °C	100	9900
I	500 °C	200	9900
J	800 °C	10	9900
K	800 °C	20	15480
L	800 °C	100	9900
M	800 °C	200	9900

III. Results and Discussions

For all process parameters except for sample G (500 °C and 10 sccm O_2) adherent, uniform coatings could be produced. On sample G, a color gradient from white to brown was macroscopically visible and delayed spallation occurred. Both effects are probably linked to a non-uniform oxygen distribution over the substrate. Dark regions indicate an oxygen deficiency and therefore the presence of ZrO_{2-x} [17]. Subsequent or delayed oxidation may have caused growth stresses which can induce spallation. To manufacture adherent uniform coatings at this parameter set, 90 sccm argon were additionally fed through the oxygen feed. More research is needed to explain why at higher substrate temperatures these problems did not arise and uniform coatings could be deposited at even lower oxygen flow rates of 5 sccm.

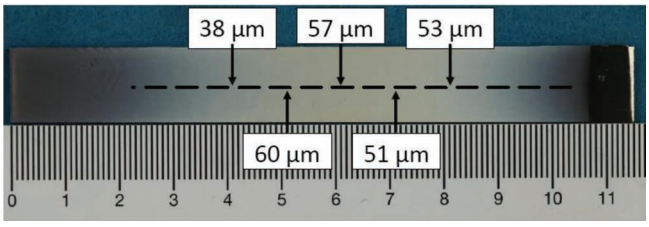

Fig. 2: Without substrate oscillation, the coating thickness varies over the substrate dropping to a few micrometers at the edges of the sample.

The aspect of coating homogeneity and non-line-of-sight character of the GFS technique was studied using duplicates of sample E. Without linear substrate oscillation, the coating thickness varies between ~ 40 and 60 µm coaxially upstream of the oven inlet (40 mm in diameter with its center at position 61 mm in Fig. 2). Zirconia was also found on the rest of the substrate although the coating thickness decreases rather fast (coating thickness in the order of a few micrometers 50 mm from the center). Nevertheless, the GFS technique can be used as a non-line-of-sight process to coat complex geometries, which was also demonstrated by Tang *et al.* [18].

With linear oscillation of the substrate the coating thickness is more homogeneous (compare Fig. 3). Over a range of 70 mm (position 15 mm up to 85 mm) there is a coating thickness of 45 ± 5 µm. Towards both ends of the substrate, the thickness drops significantly. This can be explained by the limited space in the oven, resulting in an incomplete backing out of the gas flow and in a longer staying time of the substrate middle section coaxially upstream of the oven inlet.

Although the coating differed in its thickness, no morphological differences were found in SEM images (the morphology of sample E is described later in this section).

The geometrical deposition rate varies depending on the substrate temperature and the oxygen flow rate (s. Fig. 4). The highest deposition rate of 25 µm/h is achieved for high oxygen flow rates (100 and 200 sccm) in combination with a substrate temperature of 500 °C. Since there is no decrease at 200 sccm, it can be concluded that there is no target poisoning yet. A lower oxygen flow rate of 10 sccm lowers the deposition rate to ~ 20 µm/h. Similar trends are observed for substrate temperatures of 650 °C and 800 °C. At or above 100 sccm, the deposition stays constant while lower oxygen flow rates diminish the deposition rate. Additionally, a higher substrate temperature generally lowers the deposition rate probably owing to increased surface mobility of the film-forming species resulting in less porous films.

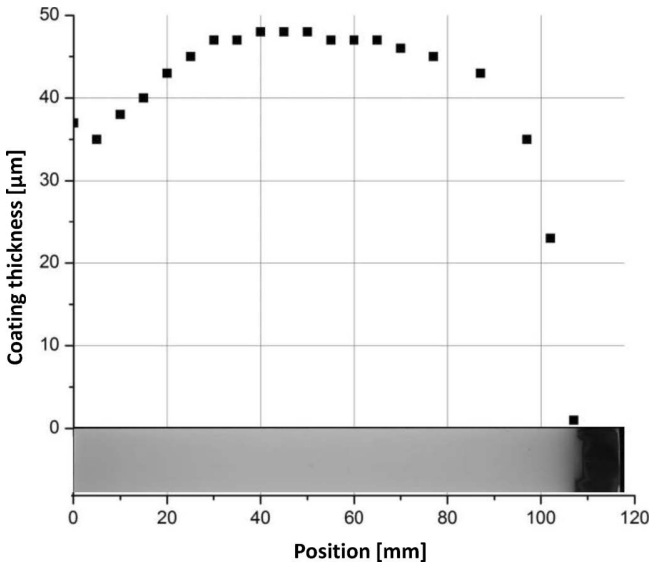

Fig. 3: With substrate oscillation, the coating thickness remains similar (45 ± 5 µm) over a wide sample region (from position 15 to 85 mm).

The achieved deposition rates in this work are in good agreement with the results of ~ 20 µm/h reported by other researchers for the reactive GFS process [16, 18, 19]. The deposition rates are an order of magnitude higher compared to conventional sputter processes (i.e. magnetron), where

the plasma region is less concentrated and the total electrical power is limited by thermal and plasma stability issues in the race track. It is – on the other hand – at least an order of magnitude lower compared to EB-PVD coatings [20], where electron guns are used with a total power of up to several 10 kW.

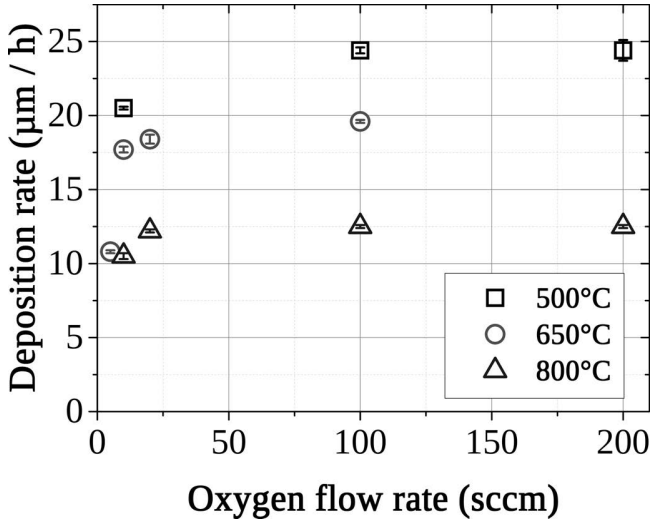

Fig. 4: Geometrical deposition rate dependent on the oxygen flow rate and substrate temperatures between 500 °C and 800 °C.

The influence of the oxygen flow rate on the microstructure of the coatings deposited at substrate temperatures of 650 °C is presented in the next paragraphs. Low oxygen flow rates (5 sccm to 20 sccm) have a different effect on the resulting microstructure than high oxygen flow rates (50 sccm to 150 sccm), compare Fig. 5. For oxygen flow rates greater than 50 sccm, all samples (D, E and F) show a similar appearance (sample F is not shown). The microstructure consists of columns that have a triangular base and a complex composition. Columns consist of thin platelets (< 100 nm) which stick out from the center at an angle. Platelets at a given height of the column form a three-sided pyramid on its tip. The structure of a column can be explained by stacking these pyramids into each other [14, 15]. Since the growth time at the column tips was shorter, the pyramids are scaled down at the tips. In addition, three ridges are present which are marked with arrows in Fig. 5 E_1 and E_3. By utilizing the focused ion beam technique, we have shown elsewhere [14, 15] that these ridges are present throughout the column (from bottom to the top and horizontally) and lie at relative angles of 120°. The feathered substructures ensure a high degree of intracolumnar porosity. It can be seen from the XRD diffractogram (Fig. 6) that a preferential grain orientation of {111} occurs, indicating that these planes are parallel to the substrate surface. Hence, the columns have a <111>-growth direction. In addition to the desired cubic/tetragonal phases, significant monoclinic fractions occur.

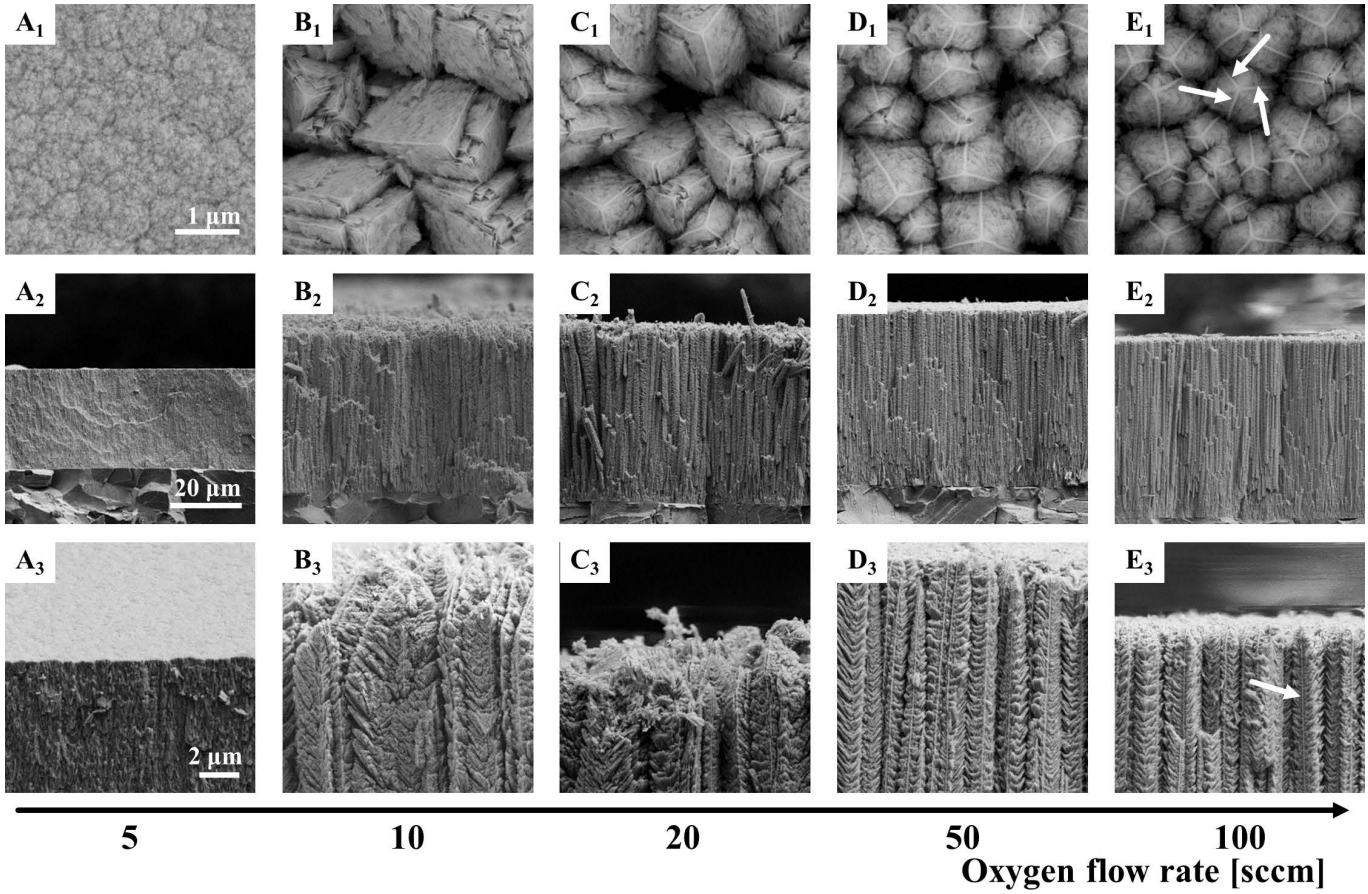

Fig. 5: SEM micrographs (A_1-E_1: top views; A_2-E_3: fracture surfaces) of GFS PSZ coatings deposited at 650 °C showing a further densification with decreasing oxygen flow rate. Sample F (150 sccm) is not shown since no difference to sample D and E was observed.

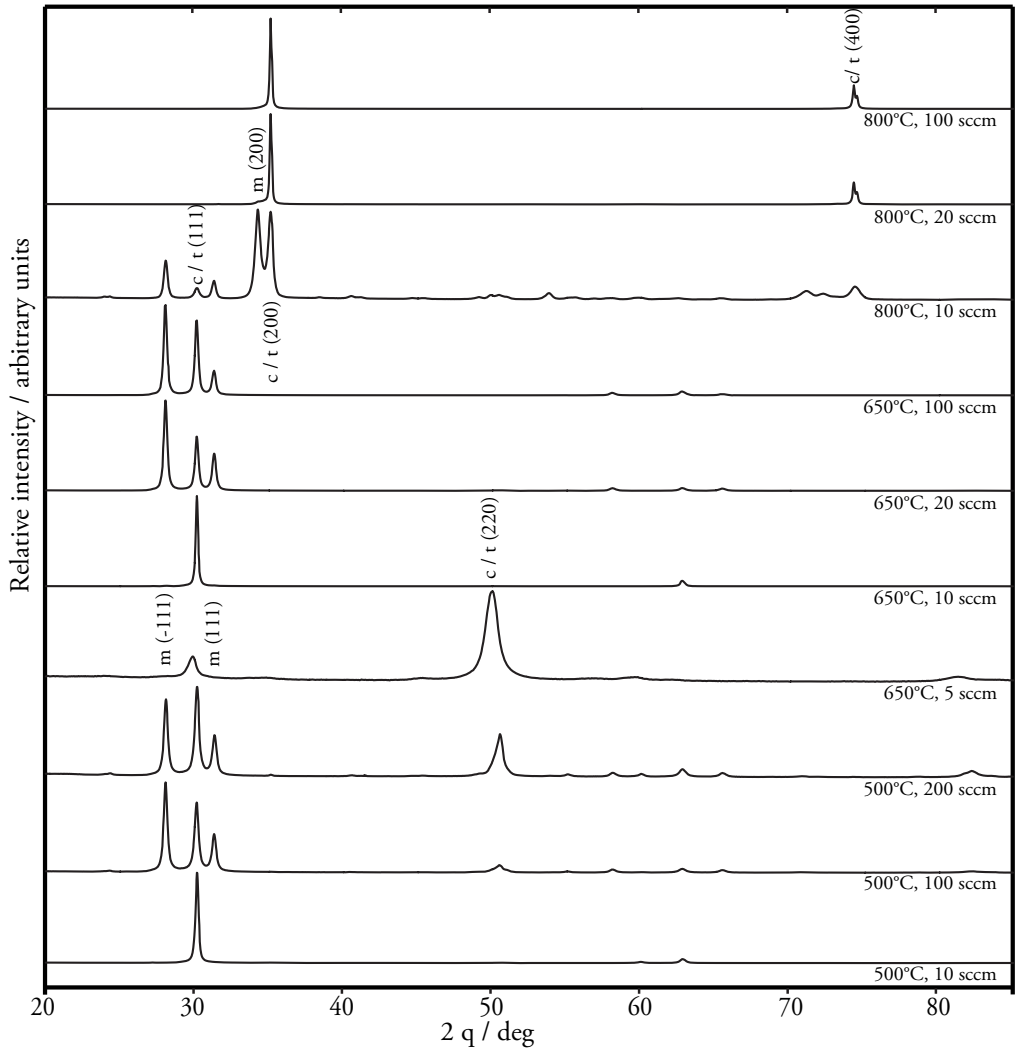

Fig. 6: X-ray diffraction patterns of GFS PSZ coatings with different substrate temperatures (500 – 800 °C) and oxygen flow rates (5 – 200 sccm) during deposition.

For oxygen flow rates of 10 and 20 sccm, the microstructures are similar to each other in the SEM images, but differ in their XRD pattern. While both coatings still exhibit a <111>-growth direction, no monoclinic fractions are visible at 10 sccm. Fig. 5 shows that single columns are still distinguishable, although they are less porous and the edges of the column tips seem more distinct. The ridges are present for both samples, but they are now in line with each corner of the triangular base of each column.

At oxygen flow rates of 5 sccm, the coating is dark and almost fully dense. Single columns are no longer distinguishable and the previously described platelet-like composition cannot be observed. There is still a preferential grain orientation, but the growth direction shifts from <111> to <220>. Owing to the dense microstructure, residual stresses were measured additionally for this specimen (and sample E for the sake of comparison) by means of X-ray stress analysis utilizing the $\sin^2\Psi$-method [21]. While at 5 sccm, compressive residual stresses in the order of 1 GPa were measured, no residual stresses were found in sample E (100 sccm).

To develop a broader understanding of how the oxygen flow rate affects the resulting microstructure, additional coatings were manufactured at substrate temperatures of 500 °C (sample G-I) and 800 °C (sample J-M), compare Fig. 7.At 500 °C, no difference between the two samples with high oxygen flow rates (H: 100 sccm and I: 200 sccm) could be observed. The columnar microstructure has the same platelet-like build-up with a triangular base that was described for coatings deposited at 650 °C (e.g. sample E). Compared to sample E, ridges are also present, but are thinner. In addition, single columns have a higher vertical distance between platelets resulting in a higher intracolumnar porosity, which corresponds with the higher geometrical deposition rate. The XRD diffractograms are also similar to sample E, and a preferential grain orientation of (111) is visible (again with monoclinic fractions). In addition, the (220) peak occurs, which is more pronounced for 200 sccm. If the oxygen flow rate is reduced to 10 sccm (sample G), the intra- and intercolumnar porosity will decrease substantially. There is almost no space between platelets and different columns, so that single columns are not easy to distinguish. The column diameter is approximately halved compared to the oxygen flow rate of 100 sccm. Despite the differences in the microstructure, the XRD pattern still exhibits a (111) preferential grain orientation, but lacks any significant monoclinic fractions.

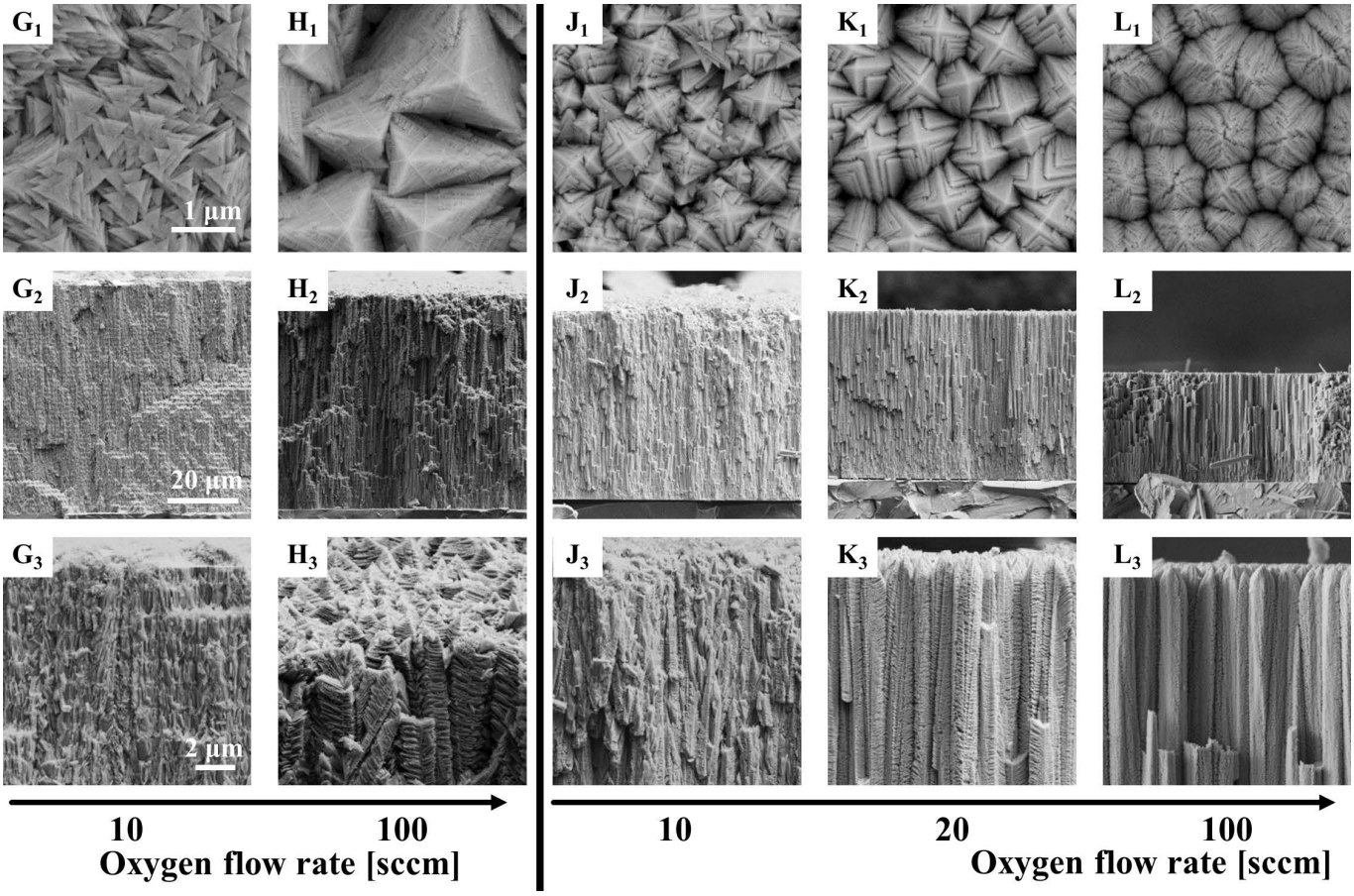

Fig. 7: SEM micrographs (G_1-L_1: top views; G_2-L_3: fracture surfaces) of GFS PSZ coatings deposited at 500 °C (sample G and H) and 800 °C (sample J-L) showing a similar densification with increasing bias voltage as seen for 650 °C in Fig. 3. Note that sample I and M (both 200 sccm) are not shown since no differences are observed to sample H and L, respectively.

At substrate temperatures of 800 °C, general trends are similar to the previously discussed substrate temperatures, although the microstructure differs. Instead of a three-fold, a four-fold symmetry is visible. At high oxygen flow rates of 100 and 200 sccm, the same microstructure is observed. Single columns are also composed of thin platelets, but they are even finer and more closely stacked, resulting in less overall porosity. In addition, no ridges are present throughout a column. Evaluating the XRD data, a clear column growth direction of <100> is visible without any monoclinic fractions. A reduced oxygen flow rate of 20 sccm leads to more distinct column tips, but neither changes the deposition rate, column diameter or XRD pattern significantly. At the lowest oxygen flow rate of 10 sccm (sample J), the microstructure is still composed of columns exhibiting a four-fold symmetry, but the column diameter is approximately halved and the porosity (inter- and intracolumnar) is greatly decreased. There is still a (100) preferential grain orientation, but additional monoclinic fractions occur.

It can be concluded from the oxygen variations that once enough oxygen is supplied to stoichiometrically oxidize the film building species, further oxygen will be pumped without affecting film growth (as long as no cathode poisoning occurs). Apparently, this is the case for oxygen flow rates ≥ 50 sccm. There seems to be a transition zone (at 20 sccm), until at further lowered oxygen flow rates (10 sccm or less), the film growth seems to be influenced by the oxygen-deficient conditions significantly. The microstructure is less porous and the deposition rate decreases, indicating subsequent oxidation.

Although the principal transport of the film-building species differs, changes in the growth direction occur also at EB-PVD coatings for different substrate temperatures. Similar changes like in this work were observed by Heydt *et al.* [22]: A transition from a <111> (700 – 950 °C) to a <100> (1150 °C) growth direction occurred, although the exact transition temperature depended on the substrate material. Further research is needed to explain the appearance or absence of monoclinic fractions at low oxygen flow rates like 10 sccm. While monoclinic fractions disappeared at both substrate temperatures that exhibited monoclinic fractions at high oxygen conditions, monoclinic fractions appeared at 800 °C where no monoclinic fractions are visible above 20 sccm.

IV. Process guidelines

It was shown that vastly different microstructures (dependent on the process parameters) can be obtained utilizing the GFS technique. The aim of this section is to evaluate these as-received microstructures as a part of the requirements needed for a future use as TBCs and to infer general guidelines for suitable process parameters. Note that although specific values are given, these may vary depending on the actual GFS source, gas flow conditions and specimen geometry.

Therefore, the main considerations are as follows:
- Coatings must be adherent and residual stresses should be avoided.
- Sufficient porosity should ensure strain tolerance and low thermal conductivity.
- Monoclinic fractions should be avoided owing to possible phase transformations.

The oxygen flow rate should be above the threshold where oxygen is in excess ("optimal" in Fig. 8), since higher flow rates do not influence the morphology. As long as cathode poisoning is prevented, excess oxygen does not affect the film morphology. Lower flow rates, on the other hand, have negative effects. Very low flow rates may result in spallation, probably due to subsequent oxidation and accompanied growth stresses ("unsuitable" in Fig. 8). Adherent coatings can be deposited at flow rates between 20 sccm and 50 sccm, but their porosity is low compared to the deposition condition under excess oxygen. In addition, it will be challenging to maintain a uniform oxygen distribution (and uniform coating morphology as well as thickness homogeneity) when coating bigger and more complex components like turbine blades. To summarize, this process window seems less favorable, and is therefore marked "with restrictions".

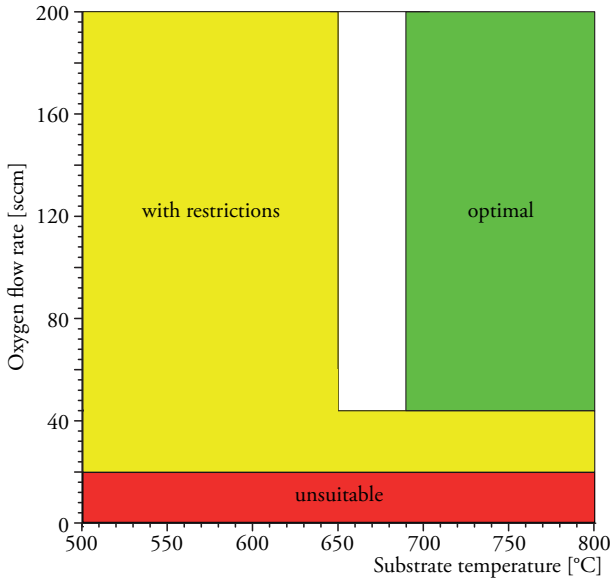

Fig. 8: Evaluation of critical process parameters (substrate temperature and oxygen flow rate) being suitable for use as thermal barrier coatings. Note that up to 650 °C monoclinic fractions occur which are absent at 690 °C. Since the temperature range between these values was not examined, that region is left blank.

Assuming no bias voltage and sufficient oxygen supply, in the studied temperature range between 500 °C and 800 °C all coatings are columnar and possess a certain degree of intracolumnar porosity enabling strain tolerance. None of these microstructures can be considered to be unsuitable *per se*, but diverging trends make further testing a necessity. With increasing substrate temperature, the adatom mobility rises and the coating becomes less porous, which is accompanied by a drop in the geometrical deposition rate of about 50 %. Accordingly, the strain tolerance should be superior and the thermal conductivity lower with lower substrate temperature. Although this favors low substrate temperatures, up to 650 °C, monoclinic fractions are present which may give rise to stresses induced by phase transformations under service conditions, resulting in coating failure. In addition, it is unclear if higher substrate temperatures lead to higher thermal conductivities. Although a higher density suggests an increase in thermal conductivity, this does not account for different pore distributions and the lack of ridges which are in line with the thermal gradient. To summarize, all substrate temperatures between 500 °C and 800 °C are suitable, but temperatures up to 650 °C are labeled "with restrictions" because of the monoclinic fraction. These are not ruled out, because it was shown elsewhere [15] that a monoclinic fraction does not necessarily result in premature failure under thermal cycling (but is still undesired).

V. Conclusions

We conclude that the GFS process is suitable for producing different microstructures based on varying substrate temperature and the oxygen flow rate:

1. If sufficient oxygen for stoichiometric oxidation is supplied (≥ 50 sccm), the microstructure will be controlled by the substrate temperature and excess oxygen is pumped without any effect (as long as target poisoning does not occur). Increasing the substrate temperature enhances surface diffusion processes of the film-building species and therefore controls the general morphology of the coating. Accordingly, with increasing substrate temperature, the microstructures become less porous and the geometrical deposition rate decreases.
2. If oxygen is deficient (≤ 20 sccm) during deposition, the microstructure will become less porous and more needlelike, probably owing to subsequent oxidation. At very low oxygen flow rates, growth stresses may induce coating spallation.
3. Several as-received microstructures were shown to be suitable candidates for thermal barrier coatings. Process parameter sets were discussed and process guidelines for the substrate temperature and the oxygen flow rate were recommended for suitable microstructures.

Acknowledgements

The authors gratefully acknowledge the financial support for the present work by the German Research Foundation (DFG), contract No. Br 2178/18 – 1, Br 2178/39 – 1, Ba 1795/6 – 1 and Ba 1795/12 – 1.

References

1 Jansohn, P. (edt.): Modern gas turbine systems: High efficiency, low emission, fuel flexible power generation. 1st edition. Woodhead Publishing Ltd, Cambridge, 2013.

2 Lechner, C.: Stationary gas turbines, in German, 1st edition. Springer-Verlag, Berlin, Heidelberg, 2003.

3 Bressers, J., Peteves, S., Steen, M.: Coatings for hot section gas turbine components. In: Fracture Mechanics: Applications and Challenges.13th European Conference on Fracture (eds. Fuentes, M., Elices, M., Martín-Meizoso, A. & Martínez-Esnaola, J.M.), **26**, 115 – 134, 2000.

4 Clarke, D.R., Oechsner, M., Padture, N.P.: Thermal-barrier coatings for more efficient gas-turbine engines, *MRS Bull.*, **37**, 891 – 898, (2012).

[5] Bürgel, R.: Handbook of high-temperature materials engineering, in German. 3rd edition. Vieweg Verlag, 2006.

[6] Azzopardi, A., Mévrel, R., Saint-Ramond, B., Olson, E., Stiller, K.: Influence of aging on structure and thermal conductivity of Y-PSZ and Y-FSZ EB-PVD coatings, *Surf. Coat. Technol.*, **177 – 178**, 131 – 139, (2004).

[7] Schulz, U., Fritscher, K., Rätzer-Scheibe, H.-J., Kaysser, W.A., Peters, M.: Thermocyclic behaviour of microstructurally modified EB-PVD thermal barrier coatings, *Mater. Sci. Forum*, **251 – 254**, 957 – 964, (1997).

[8] Schulz, U., Saruhan, B., Fritscher, K., Leyens, C.: Review on advanced EB-PVD ceramic topcoats for TBC applications, *Int. J. Appl. Ceram. Tec.*, **1**, 302 – 315, (2004).

[9] Padture, N.P., Gell, M., Jordan, E.H.: Thermal barrier coatings for gas-turbine engine applications, *Science*, **296**, 280 – 284, (2002).

[10] Pawlowski, L.: The science and engineering of thermal spray coatings. 2nd edition. Wiley, 2008.

[11] Sampath, S., Schulz, U., Jarligo, M.O., Kuroda, S.: Processing science of advanced thermal-barrier systems, *MRS Bull.*, **37**, 903 – 910, (2012).

[12] Ishii, K., Handa, S., Terauchi, H.: Sputtering of Cu in a high pressure atmosphere, *Appl. Surf. Sci.*, **33 – 34**, 1107 – 1113, (1988).

[13] Jung, T., Westphal, A.: Zirconia thin film deposition on silicon by reactive gas flow sputtering: The influence of low energy particle bombardment, *Mater. Sci. Eng. A*, **140**, 528 – 533, (1991).

[14] Rösemann, N.: Gas flow sputtered thermal barrier coatings, in German, PhD-Thesis, TU Braunschweig, 2016.

[15] Röesemann, N., Ortner, K., Petersen, J., Stöwer, M., Bäker, M., Bräuer, G., Rösler, J.: Influence of substrate temperature on morphology and behavior under cyclic thermal load of gas flow sputtered zirconia coatings, *Surf. Coat. Technol.,* **324**, 7 – 17, (2017).

[16] Rösemann, N., Ortner, K., Petersen, J., Shadow, T., Bäker, M., Bräuer, G., Rösler, J.: Influence of bias voltage and oxygen flow rate on morphology and crystallographic properties of gas flow sputtered zirconia coatings, *Surf. Coat. Technol.*, **276**, 668 – 676, (2015).

[17] Douglas, D.L., Wagner, C.: The oxydation of oxygen-deficient zirconia and its relationship to the oxidation of zirconium, *J. Electrochem. Soc.*, **113**, 671 – 676, (1966).

[18] Tang, S., Schulz, U.: Gas flow sputtering – an approach to coat complex geometries and non line of sight areas, *Surf. Coat. Technol.*, **204**, 1087 – 1091, (2009).

[19] Jung, T., Kälber, T., v. d. Heide, V.: Gas flow sputtering of oxide coatings: practical aspects of the process, *Surf. Coat. Technol.*, **86 – 87**, 218 – 224, (1996).

[20] Schulz, U.: Growth, Microstructure and lifetime of electron beam-PVD thermal barrier coating systems for turbine blades, in German, PhD Thesis, Aachen, 1995.

[21] Eigenmann, B., Scholtes, B., Macherauch, E.: Basic principles and application of X-ray stress determination in ceramics and ceramic-metal composites, in german, *Mat.-wiss. u. Werkstofftech.*, **20**, 314 – 325, (1989).

[22] Heydt, P., Luo, C., Clarke, D.R.: Crystallographic texture and thermal conductivity of zirconia thermal barrier coatings deposited on different substrates, *J. Am. Ceram. Soc.*, **84**, 1539 – 1544, (2001).